Application of IoT-based sensing and signal processing for rehabilitation

A. Moore [a], M. Mehrubeoglu*[a], Aaron Mooney[a], L. McLauchlan[b]

[a]Department of Engineering, Texas A&M Univ.-Corpus Christi, Corpus Christi, Texas, USA
[b]Department of Electrical Engineering and Computer Science, Texas A&M University-Kingsville, Kingsville, Texas, USA

ABSTRACT

IoT has emerged as a method for cloud-enabled data sharing by connecting everyday objects to the internet. Further interconnecting data transmission, IoT sensors create a network of communication among objects, sensed data, and users. This work uses an IoT development board equipped with a microcontroller to perform sensor data collection, fusion, and processing to assess the motion, flexibility, and improvements of the human knee toward the development and enhancement for a wearable sensor device. The signals are collected through simulated movements and processed through signal processing algorithms to record and analyze data that can then be used for potential therapeutic applications. To characterize the motion and its effect on the user, the three sensors targeted include inertial measurement unit (IMU), pressure, and temperature. In this paper we demonstrate an Asure cloud-based IoT environment as well as sensor data collection and fusion from simulated knee joint motion, temperature and location change.

Keywords: Internet of Things, IoT, Sensors, Wearable Sensor, IMU, temperature sensor, pressure sensor

1. INTRODUCTION

Knee injuries represent a common sports injury requiring surgery and/or rehabilitation exercises for the person to improve. In many cases, a gait laboratory to better train the muscles is utilized for treatment; these facilities can be cost prohibitive or unavailable for many possible users[1]. As part of treatment for knee injuries or for improved sports training, many researched methods identify the activity or movement performed by the person to include sitting, standing up, walking, and running[1-6]. These activities enable the movement to be corrected or improved by tracking the person's knee position. Panwar *et al.* utilize deep learning and convolutional neural network (CNN) methods to determine the type of limb movement[2]. Huang *et al.* also employ CNNs to identify the activity performed by the person[3]. Gautam *et al.* studied Long-term Recurrent Convolution networks as a means to determine the predicted type of limb movement and knee joint angle[1]. Resta *et al.* designed a wearable knee brace with a flexible sensor to take knee movement measurements[4]. Caporaso developed a wearable device to monitor knee movement to help users improve on their race-walking[5]. Penders *et al.* also developed a smart brace to aid in determining knee movements; an app gives the wearer feedback on their performed exercises for knee treatment[6].

As people age, many are affected by knee joint pain due to arthritis or other causes; Chen, Luo and Kang developed and tested a game to aid with knee joint pain improvement[7]. In other studies, an IoT-based monitoring system facilitates knee treatment for system/device users in addition to providing the ability to monitor gait and knee movement[1,8-12], especially for those individuals in remote locations or without access to treatment facilities such as gait laboratories. Amplod, Choksuchat and Sopitpan developed and studied an IoT-based wearable device that utilizes a force sensor, an inertial measurement unit, or IMU, and a gyroscope to track knee treatment for an individual[9]. Chetan *et al.* developed a wearable knee brace that is an IoT-based device that aids the user with sitting or standing via an app[10]. Dinh Phong *et al.* proposed an exoskeleton for the legs with IoT functionality built into the device[12]. Fouris et al. collected temperature data from muscles in rest and after exercise using temperature sensors[15].

*ruby.mehrubeoglu@tamucc.edu; phone 1 361 825-3378;

In this research an IoT-based device for use in rehabilitation is developed and tested on a knee model. The next section presents the setup and components of the IoT system. Section 3 shows the experimental setup and sensor data collection and fusion. Section 4 summarizes the results. Conclusions are provided in Section 5.

2. MATERIALS, TOOLS AND METHODS

Figure 1 demonstrates the conceptualization of the required IoT system components as applicable to a wearable device relevant to this project. A typical IoT system involves data acquisition through sensors and devices, and data transmission through a communication protocol. A web-based dashboard allows data access, visualization and manipulation. An IoT system requires means for analytics processing that allows data analysis and decision making for actuation, based on acquired data.

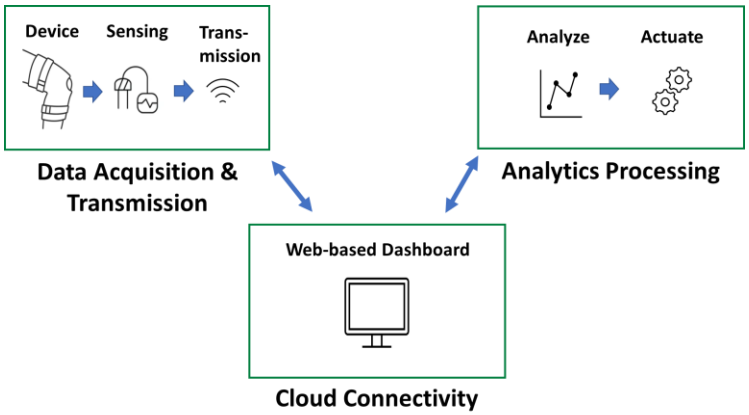

Figure 1. Conceptualization of the required components for an IoT system.

2.1 Development of the IoT system

Figure 2 demonstrates the block diagram of the developed IoT system in this project.

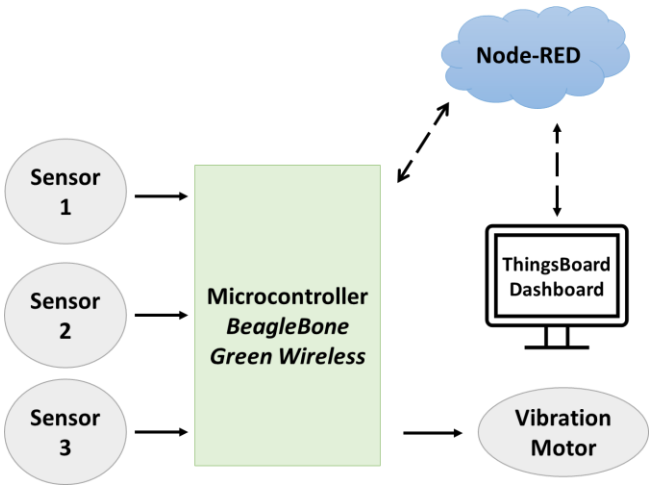

Figure 2. Block diagram for the IoT system

The diagram shows interfacing sensors with a microcontroller whose signal acquisition and processing results are then uploaded to cloud services. The sensor data fusion results are used to determine the current that is delivered to a vibration device such as a small motor, providing a customized frequency of vibration depending on the sensor data collected from the user.

In this study, an IoT Kit (Keysight U3810A) equipped with BeagleBone Green Wireless microcontroller and multiple sensors has been used for sensor interfacing and communication (Figure 3).

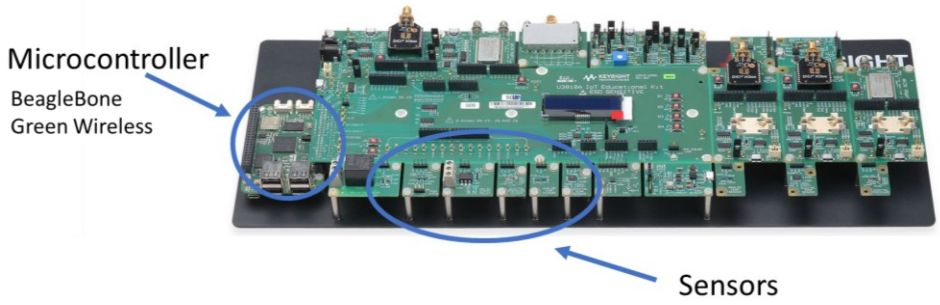

Figure 3. Keysight U3810A IoT Kit[13]

Three of the sensors available as part of the IoT kit relevant to the goals of the project were used during development for simulated data collection and sensor data fusion. The sensors used include IMU, pressure, and temperature sensors.

Flow-based programming tool, Node-RED, and open-source IoT platform, ThingsBoard, were used for data transmission over Wi-Fi to a web-based dashboard. Node-RED contains the functions that receive the sensor output data from the microcontroller and pushes that data to ThingsBoard using the IoT standard messaging protocol MQTT. In ThingsBoard, a web-based dashboard visually displays the real-time data using built-in widgets like gauges and graphs.

Figure 4 shows the IoT modular program developed on Node-RED where a connection to ThingsBoard is established and sensor data is pushed to the dashboard at a two second interval. Current functions can be expanded to push messages from Node-RED to the microcontroller for on/off operation from the dashboard, display of data history, and other data interactions customizable in the dashboard.

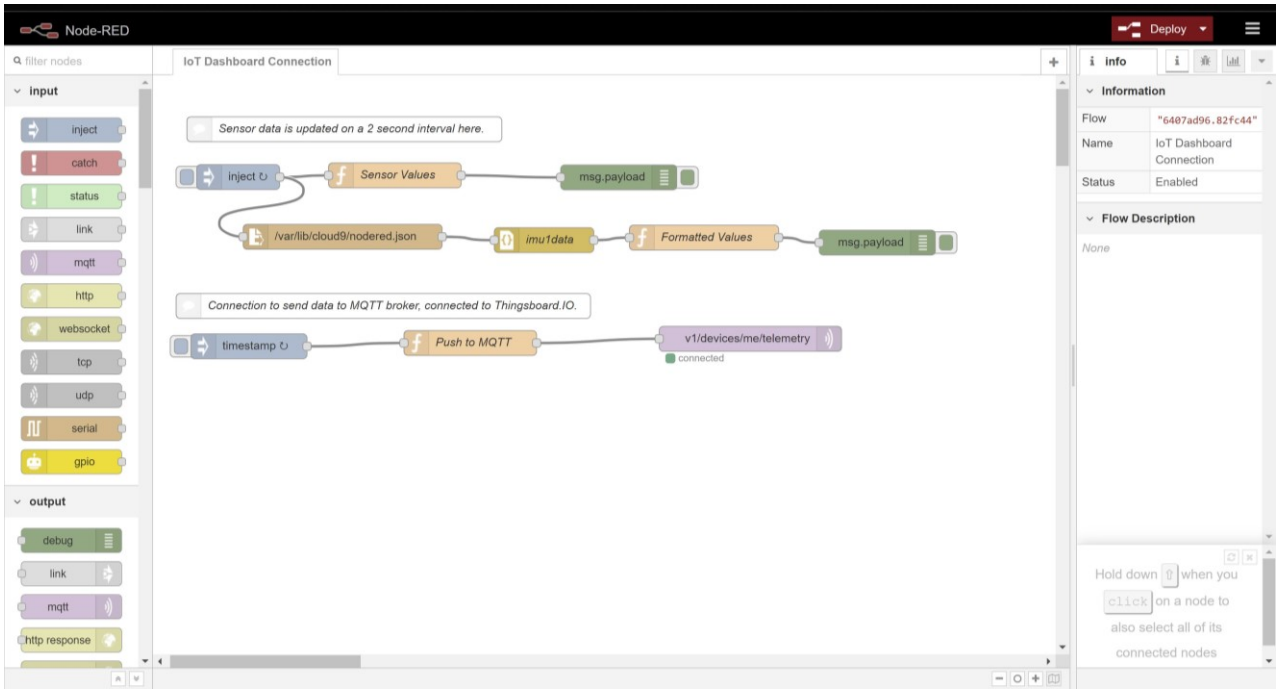

Figure 4. Node-RED flow-based coding scheme for IoT connectivity and sensor data display

2.2 Knee Model

A knee model was developed for sensor placement and testing, sensor data collection and processing through the microprocessor, and data display through the IoT dashboard as the interface. The knee model consisted of two pieces of cardboard tubes representing upper and lower leg. The two leg model pieces were connected with a wooden ball which acted as the knee joint. The three pieces were held together with rubber bands and pushpins as shown in Figure 5. The knee model was used such that the lower leg model was fixed in position such that only the upper leg model moved manually in one degree of freedom around the joint.

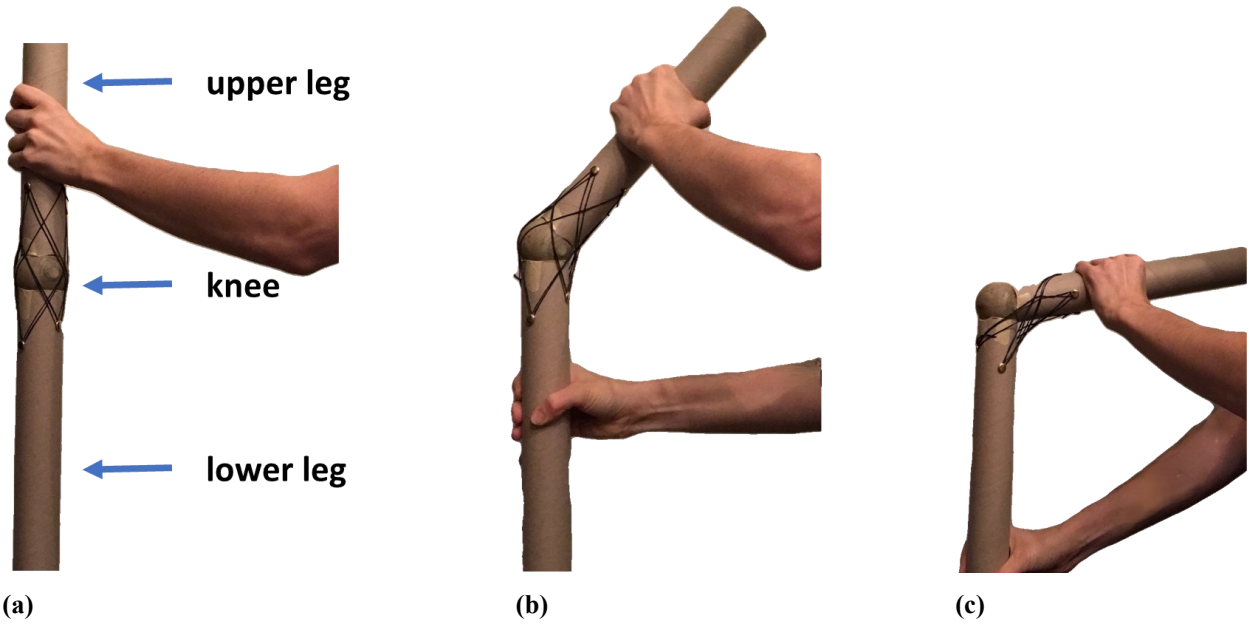

Figure 5. Knee model and simulated motion with one degree of freedom. (a) Standing; (b) Partial flexing; (c) Full or complete flexing. The three motions simulate squatting or bending at the knee at arbitrary angles by moving the upper limb of the model while the lower limb remains fixed.

The simulated motion achieved by the manual movement of the upper leg was used to generate sensor data for the IMU and pressure sensors to test the sensors and develop the IoT system before human subject testing. Temperature sensor data variations were achieved with a sock filled with warmed uncooked rice that as placed on the lower limb as displayed in Figure 6 (a). Figure 6 (a) also shows the placement of the three sensors (IMU, pressure, temperature) on the knee model. It is noted that IMU sensor captures motion parameters in 2D plane (horizontal (x) and vertical (y) axes) due to the fixed one degree of freedom of motion of the model. Figure 6 (b) demonstrates the angular motion parameters, including angular acceleration, captured by the IMU sensor.

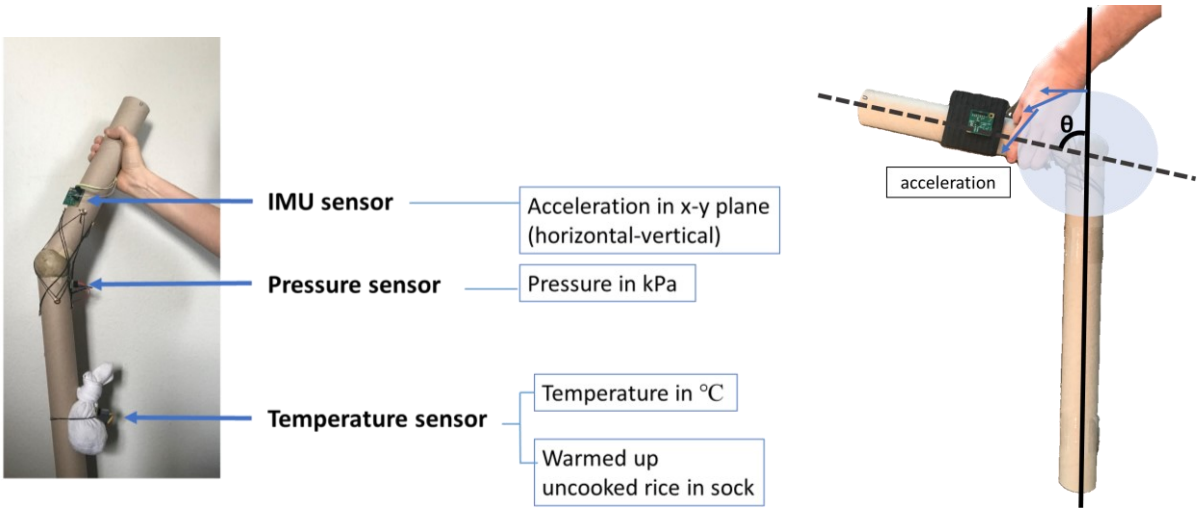

Figure 6. (a) Sensor placement on the model. Temperature changes are simulated through warmed rice placed in a sock. Pressure and IMU respond to the manually-controlled motion around the model knee joint. **(b)** Angular motion parameters captured by the IMU sensor.

3. EXPERIMENTS AND SENSOR DATA

3.1 Experiments

Figure 7 shows the collected experimental data. Each experiment consisted of four trials. Each trial was associated with sensor data collection from a simulated squat (knee flexion) after the muscles have been at rest, after the muscles have been active and were in recovery (at rest), and each of these two cases performed with complete and partial flexion or simulated squatting. Each dataset consisted of three simulated squats (knee flexion followed by extension, repeated three times).

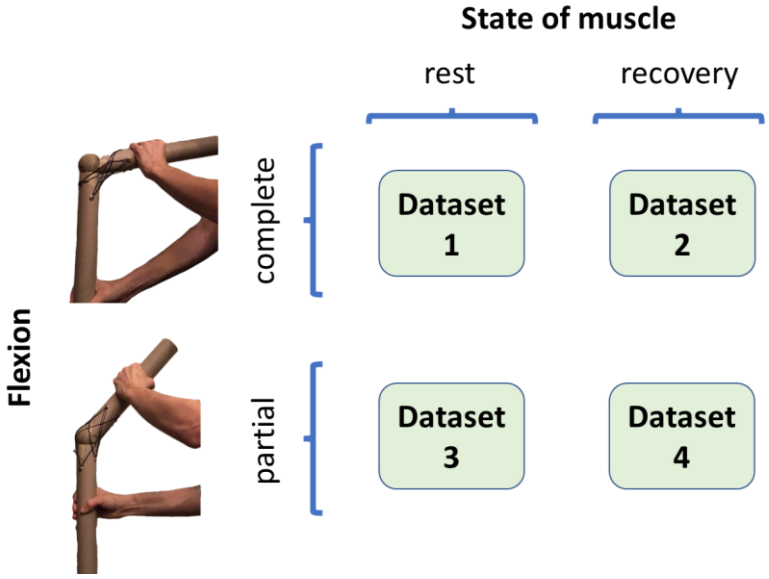

Figure 7. Collected datasets using complete flexion after muscles were in rest; complete flexion after muscles were exercised and were in recovery (rest); partial flexion after muscles were in rest; partial flexion after muscles were exercised and were in recovery (rest). For each dataset, three squats were simulated, which entailed three sets of flexing and extending the knee in the model.

Acceleration and corresponding angle from IMU sensor, L, exerted pressure (with peak pressure value, P, of interest), and temperature of muscle, T, in rest (without prior activity) and in recovery (after exercise or physical activity) were measured and recorded from the knee model.

Data was interfaced through the BeagleBone Green Wireless microcontroller, and displayed on Node-RED IoT dashboard. The microcontroller collects the raw data. Node-RED software is downloaded onto the microcontroller and connected to the WiFi. The raw data is then sent up to Node-RED. Node-RED then sends that data to ThingsBoard where the raw values are displayed in real time.

3.2 Sensor Data Fusion

Sensor fusion allows for a more robust system design as it reduces system's uncertainty. During development, sensor data fusion was achieved using a linear equation that would result in a single numerical value for decision making about the state of the muscle that can later be used for assessment, and comparative temporal analysis. Similar to the linear sensor data fusion equations described in Tan *et al.*[14], the data fusion equations used in this work for the leg muscle assessment around the knee joint, that would later be used to determine vibrational frequency for therapeutic solutions are as follows:

$$S = aL + bT + cP, \tag{1}$$

where

$$a + b + c = 1. \tag{2}$$

S is the result of sensor data fusion, and L, T, and P are the measured sensor data value from the IMU, temperature and pressure sensors, respectively. *a*, *b*, and *c* are the weights for each of the corresponding sensor data values.

To determine the output frequency, each measured sensor output is normalized between 0 and 1 before inserting to Equation (1). The normalized sensor output, X_{i_norm}, can be found using Equation (3).

$$X_{i\_norm} = \frac{X_i - X_{i\_min}}{X_{i\_max} - X_{i\_min}}, \tag{3}$$

where X_i represents individual sensor's raw output data, and *i* is the sensor index. In this case, sensor indices correspond to IMU, temperature and pressure sensors, and their output, L, T, or P, respectively. X_{i_max} represents the highest value the sensor output is expected to have for a biological system. This would be less than the manufacturer's listed upper range of the sensor. X_{i_min} represents the minimum sensor output value expected for the system. For the IMU and pressure sensors, X_{i_min} is zero. For temperature sensor, X_{i_min} is non-zero. Since each of L_{norm}, T_{norm} and P_{norm} values is thus normalized between 0 and 1, fused sensor data, S, is also between 0 and 1 due to the constraint listed in Equation (2); therefore, S_{norm} can be used as a scaling factor for the actuation input, which would determine a variable actuation current, where from Equation (1),

$$S_{norm} = aL_{norm} + bP_{norm} + cT_{norm}, \text{ and } S_{norm} \in [0,1]. \tag{4}$$

Equation (3) can be written in a scalable form to represent more than 3 sensors:

Let X_i be the actual measurement from sensor *i* where $i \in \{1, 2, 3, \ldots, n\}$ for *n* sensors. Similarly, let X_{ia} be the corresponding real or actual value of the measurement for sensor *i*, and $N_1, N_2, \ldots, i, \ldots, N_n$ be the zero mean white noise corresponding to each sensor *i*. Then, each measured sensor output value can be written as in the series of equations shown in (5) as

$$(X_1 = X_{1a} + N_1), (X_2 = X_{2a} + N_2), \ldots, (X_i = X_{ia} + N_i), \ldots, (X_n = X_{na} + N_n) \tag{5}$$

for *n* sensors. Therefore, in vector form, the measured value from each sensor can be written as

$$\mathbf{X} = \mathbf{X}_a + \mathbf{N}. \tag{6}$$

To adopt the sensor fusion algorithm[14], we will assume a combined sensor output of $\widehat{\mathrm{X}}$, where $\widehat{\mathrm{X}}$ is the estimated value for the resultant sensor fusion data as shown in Equation (7):

$$\widehat{\mathrm{X}} = \sum_{i=1}^{n} (\mathrm{X}_i \mathrm{W}_\mathrm{i}) \quad , \tag{7}$$

where W_i is the weighting factor for sensor i, or for the case presented in this paper, the values of a, b and c described in Equation (3). Same constraints as Equation (3) holds for scalable sensor system, where

$$\sum_{i=1}^{n} (\mathrm{W}_\mathrm{i}) \quad = \quad 1 \quad . \tag{8}$$

Summarizing, in our case, $n = 3$, and $\widehat{\mathrm{X}} = \mathrm{S}$.

Typically, standard deviation or variance are required to determine the weights in sensor data fusion; however, in this case, these values were set as initial conditions to $a = 0.2$, $b = 0.4$, and $c = 0.4$ to mimic the contribution of each normalized sensor output value to the sensor fusion equation.

To tailor the vibration frequency of the vibration motor shown in Figure 2, the actuation current, determined by sensor data fusion results, can be adjusted based on the vibration motor calibration to produce the current levels that will result in the desired vibration frequencies for future therapeutic applications.

Actuation current can be calculated as

$$\mathrm{I} = g\, \mathrm{S}_{norm}\, (\mathrm{I}_{max}) + d, \tag{8}$$

where I is the actuation current, I_{max} is the maximum working current allowable to the actuator, g is the gain and d is the DC offset. g and d can be found experimentally. In its simplest form, $g = 1$, and $d = 0$, simplifying the actuation current equation to:

$$\mathrm{I} = \mathrm{S}_{norm}\, (\mathrm{I}_{max}). \tag{9}$$

4. RESULTS

4.1 Sensor Data

Figures 8-10 show raw data from the three sensors placed on the knee model. Figure 8 shows the pressure sensor data from three successive simulated squats which entail flexion and extension of the upper leg while the lower leg is kept stationary and vertical. Average peak values are used as sensor output data for the sensor fusion equation described in Section 3.2. For sensor data fusion, this data is first scaled between 0 and 1 within the expected range of the peak pressure readings. Similarly, Figure 9 displays the temperature data collected over 31 seconds. This data shows increasing temperatures, as the thermal sensor adjusts to the temperature change, even though the simulated heat source is losing heat over time. This can be attributed to the response time of the sensor, and needs further investigation. IMU sensor data are plotted in Figure 10. This data shows instantaneous acceleration as the upper leg is flexed and extended three times while the lower leg is kept stationary. Green regions represent flexion, and blue regions represent extension of the knee. Acceleration information can be utilized to calculate the angular information of the muscle from the relative position of the upper and lower leg in the knee model. It is noted that the sensor output values recorded and reported here do not necessarily have biological significance and are only shown to demonstrate the operation of the sensors and expected sensor output signals.

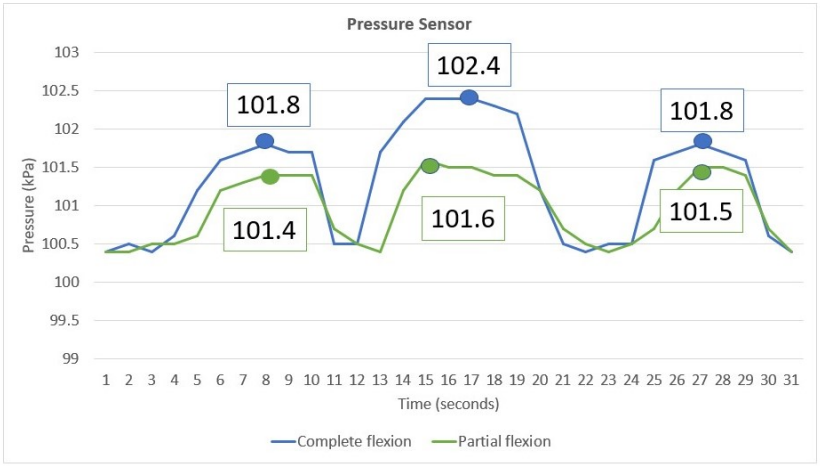

Figure 8. Pressure sensor raw data from three simulated squats, flexion-extension of the leg model. Peak pressure values indicate maximum exerted pressure. Average peak for complete flexion is 102 kPa. Average peak for partial flexion is 101.5 kPa.

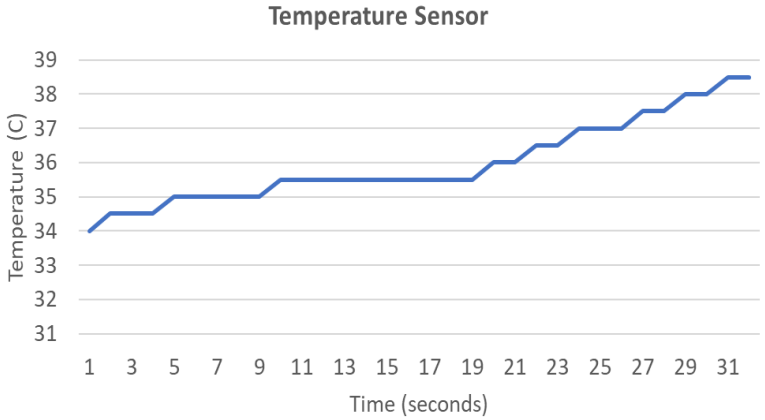

Figure 9. Temperature sensor raw data from simulated muscle heat, warmed rice in a sock, in the knee model.

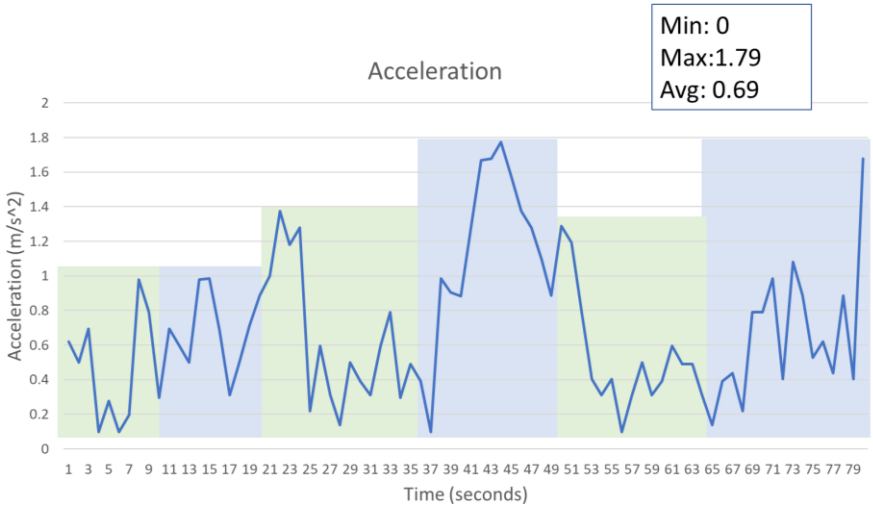

Figure 10. IMU sensor raw data from three simulated squats, flexion-extension of the leg model. This information can be used to determine angle of rotation. Average of maximum values from three simulated squats are used in the sensor fusion equation.

4.2 IoT Display

Figure 11 represents the display of sample raw data from the sensors based on the IoT interface, Node-RED and ThingsBoard. This information can be accessed remotely, and further analyzed by authorized users.

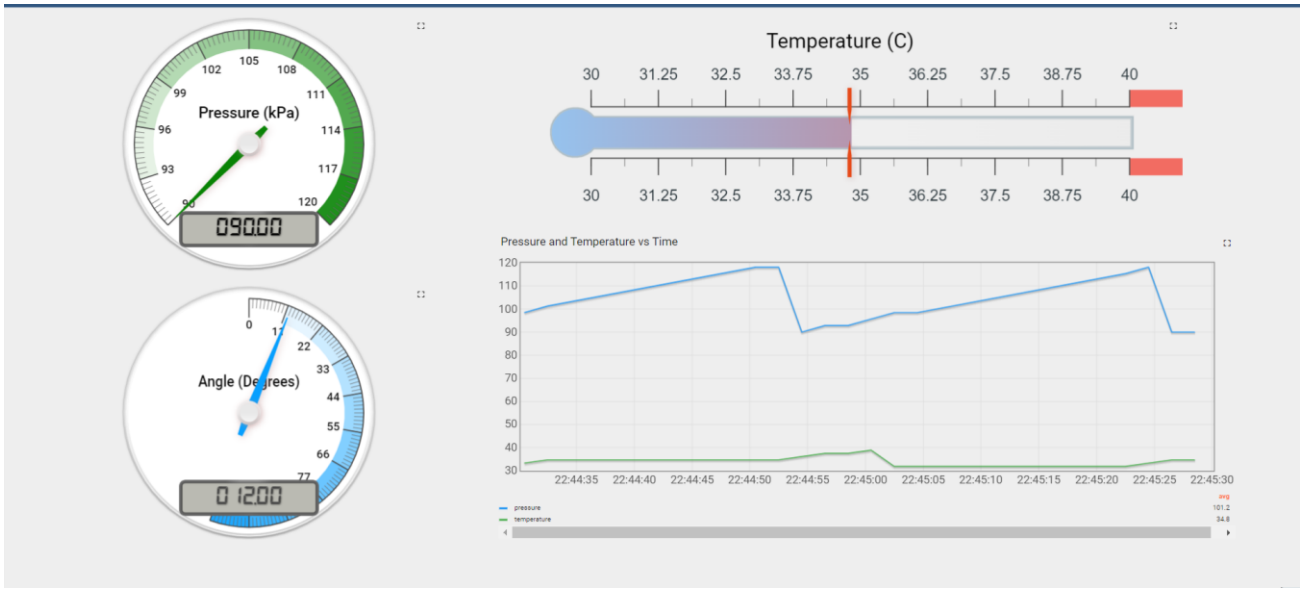

Figure 11. IoT display using ThingsBoard demonstrating individual raw IMU, pressure and temperature sensor results.

4.3 Sensor Data Fusion and Actuation

Using Equation (1), and based on interviews with a health care professional identifying sensor data and which would be of clinical contribution, the values of *a*, *b*, and *c* in Equation (4) were set to 0.2, 0.4 and 0.4, for IMU, pressure, and temperature sensor outputs, respectively, as mentioned before.

The following shows four sets of results representing four states of the muscle:

1. Muscle in rest (measurements taken without any leg exercises beforehand), full flexion (measurements taken at maximum experimental angle of the knee during simulated squatting)
2. Muscle in rest, partial flexion (measurements taken with knee at partial experimental angle of the knee during simulated squatting)
3. Muscle in recovery (measurements taken while resting after leg exercises), full flexion
4. Muscle in recovery, partial flexion

Table 1 summarizes a sample data set collected over one experiment with four states of the muscle and then normalized (L_{norm}, P_{norm}, T_{norm}), as well as calculated fused sensor data, S_{norm}, and actuation current, I.

Table 1. Sampe data set and calculations from simulated knee movement. I_{max} = 70 mA

	L_{norm} (m/s^2)	P_{norm} (kPa)	T_{norm} (^oC)	S_{norm} ($0.2L_{norm} + 0.4P_{norm} + 0.4T_{norm}$) (arbitrary units)	I (S_{norm} .(I_{max})) (mA)
1. Muscle in rest, full flexion	0.1	0.7	0.8	0.62	43.4
2. Muscle in rest, partial flexion	0.1	0.9	0.8	0.70	49.0
3. Muscle in recovery, full flexion	0.3	0.7	0.3	0.46	32.2
4. Muscle in recovery partial flexion	0.3	0.9	0.3	0.54	37.8

Although the results in Table 1 do not have any biological significance, they are important in showing the sensor data collection, as well as the computations of normalized sensor data, sensor data fusion results, and actuation current. Additional information can be communicated or saved through the IoT system through cloud services where more complex algorithms can be implemented for further analysis and decision making.

5. CONCLUSIONS AND FUTURE WORK

In this project a knee model was created to simulate leg flexion and extensions during squatting and to obtain sensor data from simulated leg muscle response. The implemented knee model was used to collect sensor data for sensing the state of a muscle during experiments. Data have been collected from sensors, and sensor fusion equation has been established. The normalized fused sensor data results determine the actuation current, or the current received by the actuator, which in turn deliver tailored vibration frequencies to the user through the vibration motor. The raw data is displayed through an IoT dashboard programmed in ThingsBoard and pushed through the cloud via Node-RED.

Future work involves fine-tuning sensor parameters from experimental data from human subjects, once IRB approval for collecting sensor data from human subjects is obtained. Addition of a second IMU to the set of sensors will improve the assessment of flexion and extension of knee, in particular, when calculating the angles. Installing the sensors on a wearable knee sensor device for human subject testing will allow collection of data for adjusting both sensor fusion equation weights, other sensor parameters, as well as actuation equation parameters from experimental data.

This device can be incorporated in future research to determine therapeutic values for actuation of vibrational frequencies deliverable by a vibration motor that is tailored to individuals. The developed model can support IoT-based data collection, analytics and actuation. Finally, once the interfacing is completed, IoT will be an excellent resource to implement machine learning and other algorithms for state of health and intervention determination from collected and analyzed data with customized interventions.

ACKNOWLEDGMENT

Materials used in this work is supported in part by the National Science Foundation under Grant No. 2044255. This project is also supported in part by the McNair Scholars Program and LSAMP Program at Texas A&M University-Corpus Christi.

REFERENCES

[1] Gautam, A., Panwar, M., Biswas, D., and Acharyya, A., "MyoNet: A Transfer-Learning-Based LRCN for Lower Limb Movement Recognition and Knee Joint Angle Prediction for Remote Monitoring of Rehabilitation Progress From sEMG," in *IEEE Journal of Translational Engineering in Health and Medicine*, 8, 1-10 (2020). Art no. 2100310.

[2] Panwar, M., Biswas, D., Bajaj, H., J'obges, M., Turk, R., and Maharatna, K., "Rehab-net: Deep learning framework for arm movement classification using wearable sensors for stroke rehabilitation," *IEEE Trans. Biomed. Eng.*, 66(11), 3026-3037 (Nov. 2019).

[3] Huang, J., Lin, S., Wang, N., Dai, G., Xie, Y., and Zhou, J., "TSE-CNN:A two-stage end-to-end CNN for human activity recognition," *IEEE J. Biomed. Health Inform.*, 24(1), 292-299 (Jan. 2020).

[4] Resta, P., Presti, D., Schena, E., Massaroni, C., Formica, D., Kim, T., and Shin, D. "A wearable system for knee flexion/extension monitoring: design and assessment," *2020 IEEE International Workshop on Metrology for Industry 4.0 & IoT*, Roma, Italy, 273-277 (2020).

[5] Caporaso, T., Grazioso, S., Panariello, D., Di Gironimo, G., and Lanzotti, A. "A wearable inertial device based on biomechanical parameters for sports performance analysis in race-walking: preliminary results," *2019 II Workshop on Metrology for Industry 4.0 and IoT (MetroInd4.0&IoT)*, Naples, Italy, 259-262 (2019).

[6] Penders, A., Octavia, J., Browaeys, H., Lauwers, G., Lefevre, S., Van Ousem, M., Saldien, J., and Verstockt, S. "SEKO: Smart System for Assisting Home-Based Rehabilitation of Knee Arthroplasty Patients," *2018 11th International Conference on Human System Interaction (HSI)*, Gdansk, Poland, 214-220 (2018).

[7] Chen, Y.-C., Luo, S.-N., and Kang, T., "Unity 3D Game for Senior's Knee Maintenance," *2020 IEEE Eurasia Conference on IOT, Communication and Engineering (ECICE)*, Yunlin, Taiwan, 269-271 (2020).

[8] Arosha Senanayake, S. M. N., and Wulandari, P., "Soft Real Time Data Driven IoT for Knee Rehabilitation," *2020 5th International Conference on Innovative Technologies in Intelligent Systems and Industrial Applications (CITISIA)*, Sydney, Australia, 1-7 (2020).

[9] Amplod, S., Choksuchat, C., and Sopitpan, S., "IoT Prototype System for Healthcare on Monitoring of Knee Osteoarthritis Treatment Patients," *2020 IEEE 2nd Global Conference on Life Sciences and Technologies (LifeTech)*, Kyoto, Japan, 303-306 (2020).

[10] Chetan, R., Avinash, N. J., Aditya, K., Gowri, M., Pranav, K. R., and Namana, (Unknown)., "Providing Knee Movement Assistance using Android and IoT," *2021 2nd International Conference on Smart Electronics and Communication (ICOSEC)*, Trichy, India, 140-145 (2021).

[11] Abdelhady, M., Elsheikh, H. E., and Ahmed, W. A., "Design a compact wireless IoT gait monitor wearable sensory system," *2021 International Telecommunications Conference (ITC-Egypt)*, Alexandria, Egypt, 1-4 (2021).

[12] Phong, L. D., Long, V. N., Hoang, N. A., and Quoc, L. H., "Development of IoT based lower limb exoskeleton in rehabilitation," *2017 14th International Conference on Ubiquitous Robots and Ambient Intelligence (URAI)*, Jeju, Korea (South), 824-826 (2017).

[13] U3810A IoT Kit, Keysight. Available: https://www.keysight.com/us/en/product/U3813A/iot-system-design-validation-training-kit-lab-sheets.html (Accessed: 20 March 2022).

[14] Tan, C., Dong, F., and Shi, Y., "Data fusion for measurement of water holdup in horizontal pipes by conductivity rings," *2011 IEEE International Instrumentation and Measurement Technology Conference*, 1-5 (2011). doi: 10.1109/IMTC.2011.5944017.

[15] Flouris, A. D., Webb, P., and Kenny, G. P., "Noninvasive assessment of muscle temperature during rest, exercise, and postexercise recovery in different environments," *Journal of Applied Physiology*, 118(10), 1310–1320 (2015).